J. Electroanal. Chem., 256 (1988) 309–326
Elsevier Sequoia S.A., Lausanne – Printed in The Netherlands

Electrochemical reactions of cyclopentadienes in non-aqueous media

Roger D. Moulton, Ramy Farid * and Allen J. Bard **

Department of Chemistry, The University of Texas, Austin, TX 78712 (U.S.A.)

(Received 26 February 1988; in revised form 8 August 1988)

ABSTRACT

Solutions of cyclopentadiene (CpH) and cyclopentadienide (Cp^-) in several non-aqueous solvents were prepared, and were examined by cyclic voltammetry. CpH shows a reduction peak in liquid ammonia at −78 °C, and also an oxidation peak at the same potential as that of Cp^- in this solvent. Bulk oxidation of CpH in liquid ammonia leads to the formation of the neutral fulvalene molecule. In THF or THF + HMPA, CpH is not electroactive. NMR studies show that ammonia is not a sufficiently strong base to deprotonate CpH. Ultramicroelectrodes were used to study the oxidation of CpH in ammonia, and the voltammetry is analyzed based on theoretical CE_qC_{2i} behavior. The synthesis of $n\text{-}Bu_4N^+Me_5Cp^-$ is described, and the electrochemistry of $MeCp^-$ is compared to the electrochemical behavior of Cp^-.

INTRODUCTION

We report here the electrochemical behavior of cyclopentadiene (CpH) and cyclopentadienide (Cp^-) in several non-aqueous solvents: liq. NH_3, tetrahydrofuran (THF), and THF + hexamethylphosphoramide (HMPA) mixtures. Non-activated conjugated dienes are generally very resistant to electrochemical reduction [1], although chemical reduction of these (especially those hydrocarbons which contain acidic protons) sometimes occurs with surprising facility [2–4]. The chemical reduction of CpH (using sodium metal) was first reported by Thiele [5] (eqn. 1) and may occur with considerable speed in ether solvents.

$$2\ CpH + 2\ Na \rightleftharpoons 2\ [Na^+Cp^-] + H_2 \qquad \Delta G^\circ \approx -170\ kJ/mol \qquad (1)$$

* Present address: Department of Chemistry, California Institute of Technology, Pasadena, CA 91125, U.S.A.

** To whom correspondence should be addressed.

0022-0728/88/$03.50

The rapid kinetics observed for eqn. (1) would intuitively appear to be associated with the high stability of the reaction products. If the stability of the products is expressed as a positive shift in the reduction potential of the diene functionality, then an electrochemical analogue of eqn. (1) (eqn. 2) would also appear to be possible.

$$2\ CpH + 2\ e^- \rightleftharpoons 2\ Cp^- + H_2 \qquad E^\circ \approx -0.95\ V\ vs.\ SHE \qquad (2)$$

Since the diene functionality of CpH is probably difficult to reduce, a mechanism involving extensive bond cleavage and rearrangement simultaneous with the electron transfer is required for the reduction to occur near the thermodynamic (reversible) potential. On the assumption that an electrochemical reduction of CpH is observable, a reaction mechanism for eqn. (2) may be obtained by an analysis of the cyclic voltammetric reduction under different experimental conditions: scan rate, concentration, pH, etc. [6]. Thus, a CV study of the electrochemical reduction of CpH may provide insight into a commonly used but poorly understood reaction. The electrochemical reduction of fluorene ($C_{13}H_{10}$) has been reported previously [7] and it was demonstrated that the anion radical of the molecule is stable under aprotic conditions, presumably due to delocalization of the added electron.

Incidental to our main motivation, other aspects of the chemistry of C_5-ring systems make them interesting to study voltammetrically. Cyclopentadienyl radicals, formed in situ by the oxidation of Cp^-, are known to dimerize rapidly and irreversibly [8]. Consequently, the cyclic voltammetry of Cp^- shows only an irreversible oxidation wave, even at relatively fast sweep rates (100 V/s). Recent advances in the fabrication of ultramicroelectrodes [9] allow for scanning at much faster sweep rates, suggesting that reversible behavior might be observed at the faster scan rates, even if the electron transfer is followed by a rapid second-order homogeneous reaction. Using the oxidation of Cp^- as an example, we will demonstrate the utility of ultramicroelectrodes in the measurement of redox potentials previously obscured by fast second-order following reactions (e.g., dimerization). In the case of Cp^-, the reversible oxidation potential is of added interest, since the carbon acidity of CpH may be calculated from it [10,11].

Finally, previous work in this laboratory [12] and elsewhere [13–17] has been directed toward the synthesis of pentafulvalenes from cyclopentadienyls. These have been used in the synthesis of new non-alternant hydrocarbons in the fulvalene series, as well as organometallic complexes [18]. The electrochemical oxidation of Cp^- represents a potentially useful method for in situ synthesis of dihydrofulvalene, which is a common intermediate in those studies. Therefore, an exploration of the anodic behavior of C_5 systems could provide details into reactivity which may be applicable to problems in synthesis.

EXPERIMENTAL

Solvents

THF solutions were prepared by vacuum distillation of the solvent from sodium benzophenone ketyl onto the predried electrolyte, as previously described [12].

HMPA was purified by distillation at 65 °C from CaH_2 under vacuum. THF + HMPA mixtures were obtained by mixing aliquots of purified THF and HMPA under N_2. The volume of the aliquots was measured in a graduated syringe. Ammonia solutions were prepared by distillation from sodium solutions, as previously described [19]. All experiments with liquid NH_3 were carried out at − 78 °C, unless otherwise specified. Experiments in other solvents were carried out under ambient conditions, except where otherwise noted.

Methods

A previously described [12] three-compartment cell was used in all the studies using conventional electrodes. A single compartment cell was used for studies with microelectrodes and electrode arrays. Several electrodes of different sizes were polished and tested at fast scan rates (v) using a ferrocene (Fc)/ferrocenium ion couple to measure the reversibility of the electrode kinetics. A well polished Pt electrode (25 μm radius) showed cyclic voltammetric waves ($\Delta E_p = 90$ mV) in MeCN + 0.1 *M* tetra-n-butylammonium tetrafluoroborate ($TBABF_4$) for v up to 10,000 V/s. The electrodes were then passed into the dry box without further polishing, and the cell was assembled with a preweighed amount of supporting electrolyte added to the chamber. After removal from the drybox, the cell was placed on a vacuum line and evacuated. The ammonia was then condensed into the cell at − 78 °C. CpH was added by syringe through a septum, or by condensation of a measured pressure of CpH vapor. The latter technique is less convenient, when exact concentrations are needed, since the volume of vapor must be known accurately. On the other hand, the purity of the solution is probably better using this method.

Chemicals

The electrolytes (potassium iodide [19] (KI), triflate [19] (KCF_3SO_3), tetra-n-butylammonium hexafluorophosphate [12]) ($TBAPF_6$) and $TBABF_4$ [12]), were prepared and/or purified by literature methods. CpH and methylcyclopentadiene were cracked from the dimers at 160 °C. 1,2,3,4,5-Pentamethylcyclopentadiene (Aldrich) was distilled under vacuum prior to use. Potassium butoxide (Alfa) was used without further purification. Sodium cyclopentadienide · dimethoxyethane (NaCp · DME) was prepared from Na dispersion (40% in oil) and freshly cracked CpH as previously described [20]. Potassium 1,2,3,4,5-pentamethylcyclopentadienide · dimethoxyethane (KMe_5Cp · DME) was prepared by literature methods [21]. Lithium cyclopentadienides were prepared by the addition of n-BuLi (1.4 *M* in hexane) to a stirred − 78 °C solution of the cyclopentadiene in ether. The resulting precipitate was filtered under nitrogen, washed with dry degassed hexane, and dried under vacuum.

Synthesis of tetra-n-butylammonium 1,2,3,4,5-pentamethylcyclopentadienide (TBA^+ Me_5Cp^-)

KMe_5Cp · DME (0.41 g, 1.55 mmol) was added to a 100 ml Schlenk flask, and 50 ml THF was distilled onto it under vacuum. The resulting slurry was stirred rapidly

as $TBAPF_6$ (0.55 g, 92 mol %) was added to it against a counter current of nitrogen. The yellowish KMe_5Cp immediately disappeared and was replaced by a finely divided white powder. The solution was stirred for 1 h, and was then allowed to settle. The powder was removed by decanting the solution. The volume of the THF was then reduced to 10 ml, which resulted in the precipitation of a white powder. The powder was collected by decanting, washed three times with dry, deaerated pentane, and then dried under vacuum. The yield of the product $TBA^+Me_5Cp^-$ by this method is ~ 90%. ^1H NMR (CD_3CN): δ 0.97 (m, 20 H, $(N-(CH_2CH_2C\underline{H}_2C\underline{H}_3)_4)^+$), 1.47 (m, 8 H, $(N-(CH_2C\underline{H}_2CH_2CH_3)_4)^+$), 1.77 (br s, 15 H, Me_5Cp^-), 3.10 (m, 8 H, $(N-(C\underline{H}_2CH_2CH_2CH_3)_4)^+$).

Equipment

Voltammetric measurements at scan rates below 5 V/s were carried out with the potentiostatic equipment as described previously [22]. Studies with ultramicroelectrodes were carried out with a homemade potentiostat with data acquisition on a Norland Model 3001 processing digital oscilloscope, as described in more detail elsewhere [23]. Potentials in THF and THF + HMPA are reported vs. SHE by reference to ferrocene/ferrocenium [24,25]. In ammonia the silver wire QRE has a reproducible potential (of + 2.3 V vs. electron injection [19]), so all electrode potentials in ammonia are reported vs. this reference electrode. NMR experiments were performed on a 200 MHz Nicolet NT-200 instrument.

RESULTS AND DISCUSSION

Reduction behavior

A NH_3 + 0.1 *M* KI solution showed a clean background, with no reduction waves positive of solvated electron injection (Fig. 1a). Condensation of CpH vapor into the cell resulted in the appearance of a reduction wave close to the solvent limit. When a Pt working electrode was used, the shape of the wave was irregular (Fig. 1b), suggesting non-diffusional mass transfer in solution (such as occurs, for example, when a gas is evolved at the electrode). At a W electrode, a more conventional reduction was observed, at a more negative potential, relative to Pt (Fig. 1c). At either electrode, the reduction was electrochemically irreversible and no anodic peak corresponding to the oxidation of the anion radical of CpH was seen even at high scan rates (e.g., 10 V/s).

In contrast to the results in liq. NH_3, a solution of CpH in THF showed no cathodic wave prior to the solvent limit. Since the accessible potential windows of these two solvents are similar, a reduction would have been observable in THF, if one had occurred at the same potential as in ammonia. The absence of a reduction in THF suggests that solvation effects play a major role in the heterogeneous electron transfer. If the reduction of CpH in liq. NH_3 was simply due to its diene functionality, it would be difficult to rationalize a solvent effect as pronounced as that observed between THF and NH_3. However, the difference can be attributed to a preceding acid–base equilibrium. CpH is an unusually strong carbon acid (aque-

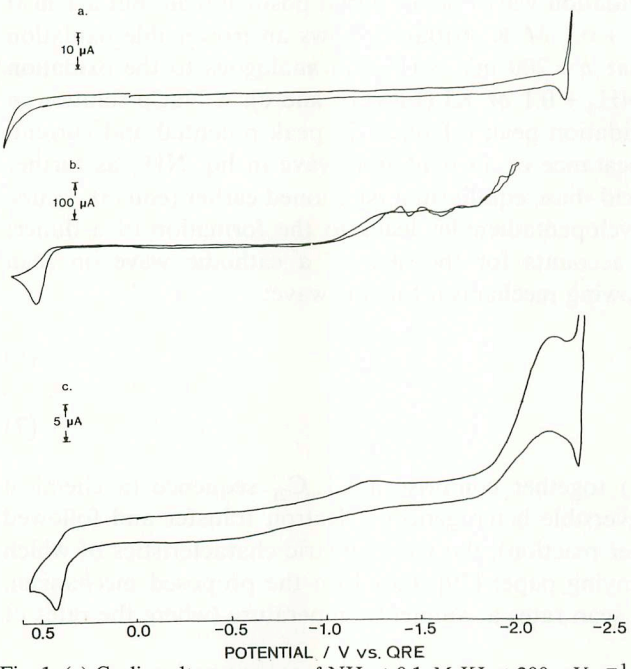

Fig. 1. (a) Cyclic voltammogram of $NH_3 + 0.1\ M$ KI at 200 mV s^{-1}. Potential axis is listed with respect to a Ag QRE, which had a reproducible potential of +2.3 V vs. e^-. (b) Cyclic voltammogram of 0.14 M CpH in $NH_3 + 0.1\ M$ KI using a Pt working electrode ($A = 0.001$ cm^2). Scan rate = 200 mV s^{-1}. (c) Cyclic voltammogram of 5 mM CpH in $NH_3 + 0.1\ M$ KI with a W working electrode ($A = 0.0083$ cm^2). Scan rate = 200 mV s^{-1}.

ous $pK_a \approx 16$ [26]), while ammonia can act as a base ($pK_b \approx 11$). If a proton transfer reaction takes place between the CpH and NH_3, the reduction wave at Pt can be attributed to the presence of ammonium ion in solution. The influence of the overpotential of the reduction process on the electrode material agrees with this assignment, since Pt is known to catalyze proton reduction more effectively than W in ammoniacal solution [27]. The electrochemical reduction of CpH in Fig. 1 may be compared to the previously reported [28] electrochemical reduction of NH_4^+ in liq. NH_3 at Pt, which occurs at the same potential. Therefore, we propose the following mechanism for the reduction of CpH in ammonia:

$$CpH + NH_3 \underset{k_{-1}}{\overset{k_1}{\rightleftharpoons}} NH_4^+ Cp^- \qquad K_1 = k_1/k_{-1} \tag{3}$$

$$NH_4^+ Cp^- + e^- \rightarrow NH_3 + H^\cdot + Cp^- \tag{4}$$

$$H^\cdot \rightarrow 1/2\ H_2 \tag{5}$$

Oxidation behavior

CpH in THF shows no oxidation waves on an initial positive scan, but a 1 m*M* solution of CpH in liq. $NH_3 + 0.1$ *M* K^+triflate$^-$ shows an irreversible oxidation peak at 0.41 V vs. Ag/Ag^+ at $v = 200$ mV/s (Fig. 2) analogous to the oxidation waves seen on Pt and W in $NH_3 + 0.1$ *M* KI (Figs. 1b and c). A NaCp solution in ammonia shows a similar oxidation peak (identical in peak potential and current, see below). We take the appearance of an oxidation wave in liq. NH_3 as further evidence that the preceding acid–base equilibrium mentioned earlier (eqn. 3) occurs. The chemical oxidation of cyclopentadienides leads to the formation of a dimer; this fast following reaction accounts for the lack of a cathodic wave on scan reversal. We propose the following mechanism for this wave:

$$NH_4^+Cp^- - e^- \underset{k_b}{\overset{k_f}{\rightleftharpoons}} NH_4^+ + Cp^\cdot \tag{6}$$

$$2\ Cp^\cdot \xrightarrow{k_2} (\text{dihydrofulvalene}) \tag{7}$$

Equations (3), (6) and (7) together comprise a CE_qC_{2i} sequence (a chemical reaction preceding a quasi-reversible heterogeneous electron transfer and followed by an irreversible second-order reaction), the voltammetric characteristics of which are discussed in an accompanying paper [29]. Based on the proposed mechanism, one would expect that at low scan rates at ambient temperature (where the rates of

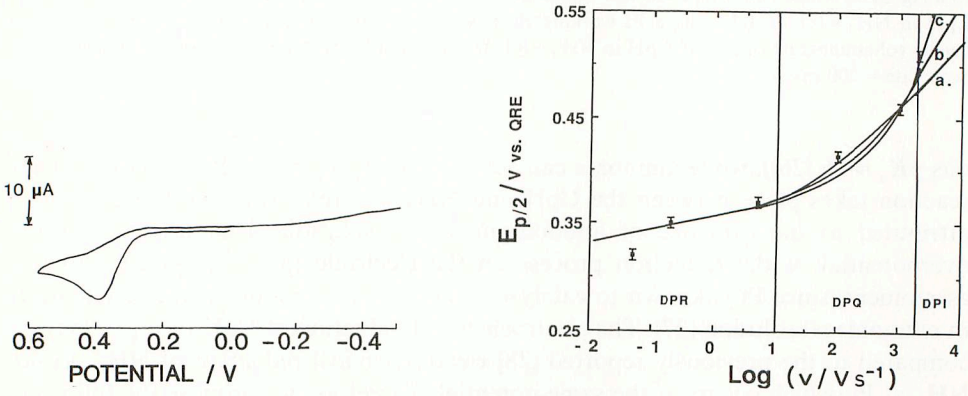

Fig. 2. Cyclic voltammogram for oxidation of 1.0 m*M* CpH in $NH_3 + 0.1$ *M* K^+ triflate$^-$ (oxidative scan), at a W electrode. Scan rate = 200 mV s^{-1}.

Fig. 3. Half peak potential vs. log v for the CV oxidation of CpH in $NH_3 + 0.1$ *M* K^+ triflate$^-$. CVs at and below 2 V s^{-1} were carried out using a W electrode. Faster scan rates were obtained with a Pt ultramicroelectrode (see Experimental). DPR, DPQ, and DPI depict diffusion-controlled behavior with reversible, quasi-reversible and totally irreversible heterogeneous kinetics, as described in ref. 29, and the working curves of peak potential vs. log v were adapted from those presented for the CE_qC_{2i} mechanism. (a) $v^{1/2}k_{HE} = 10$; $(1-\alpha)n = 0.11$; (b) $v^{1/2}k_{HE} = 7$; $(1-\alpha)n = 0.20$; (c) $v^{1/2}k_{HE} = 3.5$; $(1-\alpha)n = 0.32$; where $k_{HE} = \Lambda K_1^{(1-\alpha)}$.

eqns. 3, 6 and 7 are very fast relative to the scan rate) the half-peak potential would shift 20 mV with each ten-fold change in scan rate, and $i_{pa}/v^{1/2}$ would be constant. The ratio i_{pc}/i_{pa} is small, if the dimerization reaction is fast. As the scan rate is increased, several changes could be observed, depending on which reaction becomes rate-determining. If the preceding reaction (eqn. 3) becomes the slow step, $i_{pa}/v^{1/2}$ becomes scan rate dependent and decreases with increasing v. If the heterogeneous kinetics (eqn. 6) become rate-determining, the shift in half-peak potential with v would increase from 20 mV per scan rate decade to $30/(1-\alpha)n$ mV (where $(1-\alpha)$ is the anodic transfer coefficient). If the dimerization were the slow step, a reduction peak on the negative scan would be observed, and the half-peak potential would be independent of scan rate (i.e., it would follow a CE_q mechanism).

We will show in the following discussion that the species dubbed $NH_4^+Cp^-$ is not ionic, but is rather a tightly associated ammonia–CpH complex. The Nernst equation for eqn. (6) based on a non-ionic $NH_4^+Cp^-$ is:

$$E = E^{\circ\prime} + (RT/nF)\log([NH_4^+][Cp^\cdot]/[NH_4^+Cp^-]) \qquad (8)$$

Since our solution was not buffered, the reaction depicted in eqn. (6) is formally bimolecular in the reverse direction. A consequence of this stoichiometry is a degree of broadening in the CV (or polarographic) waveshape relative to a simple $A + e^- \rightleftharpoons B$ case (with unimolecular stoichiometry). However, at 50 mV s^{-1} we observe $E_{3/4} - E_{1/4} = 48$ mV for the oxidation of CpH in ammonia, which is only slightly larger than the value of 42 mV predicted for a wave in the DPR zone of the CE_qC_{2i} mechanism when the electron-transfer step produces a single product [29]. This suggests that "adventitious" proton donors in solution buffer the solution to some extent so that the reaction in eqn. (6) is pseudo-first-order in both the forward and reverse direction. Questions concerning the stoichiometry of eqn. (6) do not alter the dependence on scan rate of the peak potential and current, since the rates of preceding and following reactions are not affected by the presence of proton donors in solution.

A plot of half-peak potential vs. log v is given in Fig. 3. At scan rates below 10 V s^{-1}, the slope $\Delta E_{p/2}/\Delta \log v$ is 20 ± 8 mV, suggesting that the reaction in eqns. (3), (6) and (7) are all fast at this sweep rate. At $v \geqslant 100$ V/s, quasi-reversibility in the heterogeneous electron-transfer becomes important, and the slope increases to values above 60 mV. Up to scan rates of 2000 V/s the oxidation wave remains irreversible, and no reduction is seen on the negative scan. Thus the following reaction (eqn. 7) remains fast, even at this sweep rate. $i_p/c^\circ Av^{1/2}$ is essentially constant (Fig. 4) throughout the range, which also suggests that the reaction in eqn. (3) remains essentially at equilibrium at all scan rates (i.e., $\lambda_1 K_1^2 > 10^{1.4}$ ($\lambda_1 = nF(k_1 + k_{-1})/RTv$) [29]).

Bulk electrolysis results

To substantiate the electrochemical mechanism outlined above, controlled potential oxidations of CpH and Cp^- solutions in NH_3 were carried out. In both cases, oxidation at a Pt electrode at $E_{app} = +0.5$ V lead to rapid electrode fouling and

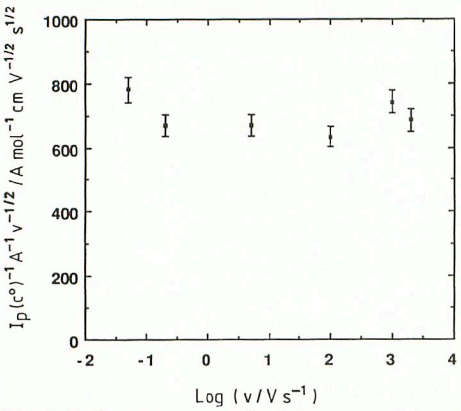

Fig. 4. Peak current normalized to concentration, electrode area and the square root of scan rate vs. log v for the oxidation of CpH in NH_3 + 0.1 M K^+ triflate$^-$.

passivation, but in concentrated solutions, several coulombs could be passed before the oxidation process ceased. At this point, the solution had changed in color from colorless to dark red.

The appearance of this solution closely resembled that of a solution of Cp^- exposed to O_2, where the color results from autoxidation of Cp^- and is due to the formation of the neutral fulvalene molecule [16]. Thus, we propose the ultimate formation of fulvalene during the oxidation of CpH or Cp^- in ammonia (eqn. 9).

$$CpH - 4\ e^- - 4\ H^+ \rightarrow \text{fulvalene} \qquad (9)$$

It is known that initially, dihydrofulvalene is formed during the oxidation, as shown in eqn. (7). The formation of fulvalene can be accounted for by a deprotonation by the solvent to the fulvalene dianion, which may then be oxidized to the neutral form at the applied electrode potential. An analogous pathway was postulated [16] to account for fulvalene formation following autoxidation of Cp^-. No attempt at isolation of fulvalene or dihydrofulvalene was made, since both have been shown [13,20] to polymerize in concentrated solution. In fact, polymerization of these species is probably involved in the electrode fouling process, since a relatively high concentration of the monomeric forms would be found near the electrode surface. If the polymer is formed in the diffusion layer, it may later precipitate onto the electrode surface. On the other hand, a fraction of the neutral fulvalene does not polymerize, and apparently escapes into the bulk solution. The anodic electrolysis of CpH in liquid ammonia thus represents a convenient, one-pot synthesis of small quantities of this uncommon molecule.

A voltammogram of the red solution prepared by electrolysis of Cp^- in ammonia is shown in Fig. 5. A new reversible redox process appears at $E_{1/2} = -0.30$ V, which may represent the reduction of the colored material. This is in contrast to the behavior shown in Fig. 2, in which no reducible species is formed initially following the oxidation of CpH in ammonia. Therefore, the red material is produced slowly

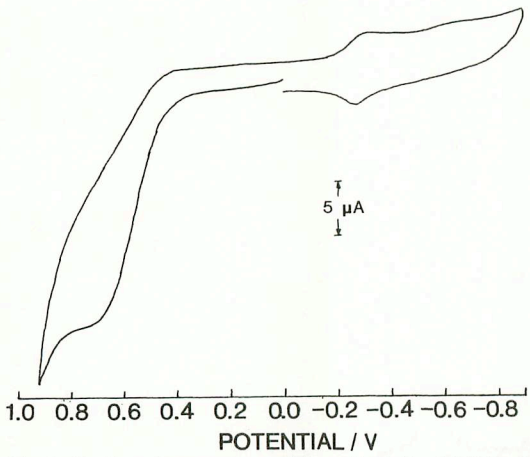

Fig. 5. Cyclic voltammogram of 1 m*M* NaCp·DME in NH_3 + 0.1 *M* K^+ triflate$^-$ after bulk electrolysis at $E_{app} = +0.5$ V.

on the bulk electrolysis time scale but not during a CV scan. Thus, the previous discussion of the kinetics based on the CE_qC_{2i} mechanism remains valid, since the additional reaction is slow. Of course, since no evidence for the formation of the red material is observed on the CV timescale, a detailed mechanism of the evolution of neutral fulvalene cannot be obtained.

NMR studies

The NMR spectrum of 0.1 *M* CpH in ammonia at − 40 °C is shown in Fig. 6a. Two groups of resonances are observed: a quintet ($J = 1.31$ Hz) can be assigned to the pair of aliphatic protons ($\delta = 2.13$); a multiplet at lower field can be assigned to the two pairs of vinylic protons ($\delta = 5.64, 5.73$). The integration of the aliphatic and vinylic groups is in the ratio 1 : 2. This can be contrasted to the NMR spectrum of CpH in acetone at − 40 °C (Fig. 6b), in which the spectrum is similar (although the aliphatic and vinylic resonances are separated by an additional 0.2 ppm) and in both cases the spectra imply a flat ring structure of CpH (C_{2v} symmetry). A detailed interpretation of the NMR spectrum of CpH has been described previously [30].

The NMR spectrum in Fig. 6a can also be interpreted to demonstrate that the electrochemical results cannot be attributed to the formation of an ionic $NH_4^+Cp^-$ structure (with a C_5-ring geometry analogous to Na^+Cp^-) formed from CpH in ammoniacal solution. A previous study of a mixture of CpH and Cp^- in ammonia has shown that resonances for each species in solution can be observed [31]. A high concentration of an ionic species can be ruled out, since the spectrum does not show evidence for Cp^- (i.e., a singlet 0.9 ppm upfield of the vinylic protons). Under the conditions employed in the NMR experiment, a 1 m*M* concentration of Cp^- would certainly have been observable, so the equilibrium constant for the formation of an ionic species must be less than 0.01. On the other hand, while the NMR spectrum

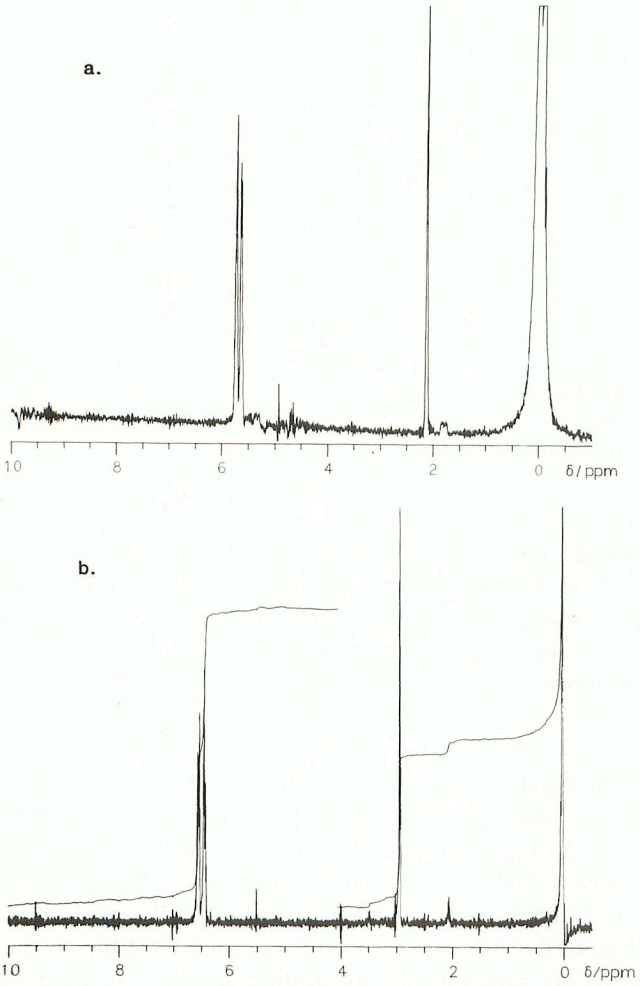

Fig. 6. (a) 200 MHz NMR spectrum of 0.1 *M* CpH in NH_3 at $-40\,^{\circ}$C. Proton shifts are reported relative to NH_3. The "peak" at $\delta = 4.90$ is an artifact of the data acquisition. (b) NMR spectrum of 0.1 *M* CpH in d^6-acetone. Proton shifts are reported relative to TMS.

does not rule out a lower concentration of the ionic form, this would not be consistent with the observed behavior of the electrochemical oxidation wave. As mentioned previously, the peak current measurements at high scan rates suggest the equilibrium is rapid ($\lambda_1 K_1^2 > 10^{1.4}$). If $K_1 \leqslant 0.01$ and $v = 2000$ V s^{-1}, this implies $k_1 \geqslant 1.3 \times 10^5$. Since the reaction in eqn. (3) represents a means by which all the protons in CpH may be interchanged, a rapid equilibrium for the reaction involving an ionic species would coalesce the aliphatic and vinylic resonances to a single peak. Coalescence would be observed for a scheme involving ionic species when $k_1 >$

$(\pi\sqrt{2}/2)(\nu_{\text{aliphatic}} - \nu_{\text{vinylic}}) = 1500\ \text{s}^{-1}$. The spectrum in Fig. 6a contains more than one line; therefore, an ionic form of $NH_4^+Cp^-$ in low concentration can be ruled out as the electroactive species, since the preceding reaction (eqn. 3) cannot be slow on the NMR time scale and fast on the CV timescale under identical conditions.

An alternative structure, in which the solvent becomes associated with the aliphatic protons, is illustrated in eqn. (10):

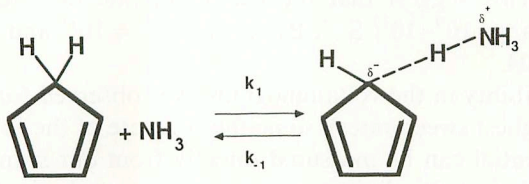

(10)

($K_1 = k_1/k_{-1}$). In our formulation, the formation of the electroactive species involves the polarization of the aliphatic C–H bonds of CpH by an interaction with the solvent. The interaction leads to increased electron density on the α-carbon, which in turn results in the appearance of the oxidation wave. The aliphatic protons will not become scrambled with the vinylic protons as long as the C–H bond remains intact in the reaction illustrated in eqn. (10). For the protons to appear equivalent on the NMR timescale (and to explain the electrochemical results), the reaction in eqn. (10) must be rapid.

Rate constants and redox potential determinations

The rate of the heterogeneous electron-transfer, as well as limits on the homogeneous rate constants can be obtained from the voltammograms. With these estimates, a range of possible values of the reversible potential for oxidation for the $NH_4^+Cp^-/Cp^{\cdot}$ couple can be found. The electron-transfer rate constant and the transfer coefficient $(1-\alpha)n$ were estimated by fitting the half-peak potential data (Fig. 3) to the working curves for the CE_qC_{2i} case presented previously [29]. An alternative approach is to estimate the transfer coefficient independently (for example, from the value of $E_{3/4} - E_{1/4}$ at the highest scan rate), and adjust the working curve for this value to the data to obtain the heterogeneous electron-transfer rate constant.

For the oxidation of CpH in ammonia, totally irreversible heterogeneous electron transfer was only approached at 2000 V s^{-1}. Therefore, the value of $(1-\alpha)n$ obtained from the waveshape at this sweep rate may not be accurate. By applying the expression [29] $E_{3/4} - E_{1/4} = 39/(1-\alpha)n$ ($= 130$ mV at 2000 V s^{-1}), an upper limit of $(1-\alpha)n = 0.30$ is obtained. A set of working curves of $E_{p/2}/\log v$ were generated with this value and two smaller values of $(1-\alpha)n$, and are overlaid on the data in Fig. 3. The rate constant for the heterogeneous electron-transfer reaction was then adjusted for each curve to achieve the best fit to the data. Due to the scatter in the data a relatively large uncertainty exists in the values obtained by this

procedure: $(1-\alpha)n = 0.22 \pm 0.11$; $v^{1/2}k_{HE} = k^\circ(D_A/D_B)^{(1-\alpha)/2}K_1^\alpha(D_A RT/F)^{-1/2} = 7 \pm 4$ $V^{1/2}$ $s^{-1/2}$, where D_A and D_B represent the diffusion coefficients of $NH_4^+Cp^-$ and $Cp^\cdot$, respectively.

Purely diffusional currents (constant $i_p/v^{1/2}$ as shown in Fig. 4) were observed for the oxidation of CpH in liquid ammonia at all scan rates. This implies [29] that $\lambda_1 K_1^2 > 10^{1.4}$ (where $\lambda_1 = nF(k_{-1}+k_1)/RTv$). A lower limit for the equilibrium constant can be obtained, if a value of λ_1 is available. Estimates of the rates of solvolysis of strong acids suggest that the maximum rate of a reaction with the solvent [32] is in the range 10^9–10^{11} S^{-1}. By setting $k_{-1} = 10^{11}$ and $v = 2000$ V s^{-1}, we find that $K_1 > 0.004$.

No chemical reversibility in the voltammograms was observed for the CpH/NH_3 system (even at the highest sweep rates), so neither the rate of the following reaction k_2 nor the redox potential can be measured directly from our scans. However, the maximum possible value of the dimerization rate constant k_2 is governed by the diffusion-controlled lifetime of the cyclopentadienyl radical. The maximum value k_2 may attain is the diffusion-controlled limit [33]:

$$k_{2(\mathrm{diff})} = 8RT/(3\times 10^3)\eta_{(-78)}\ M^{-1}\ s^{-1} \tag{11}$$

$\eta_{(-78)}$ (the viscosity of liquid ammonia at $-78\,^\circ C$, which was the temperature used for the electrochemical studies) can be calculated by extrapolation from values at higher temperatures [34]. Assuming the influence of the supporting electrolyte (0.1 *M* KI) on the viscosity is negligible, we estimate $\eta_{(-78)}(NH_3 + 0.1\ M\ KI) = 0.0055$ poise (1 poise $= 10^{-1}$ Pa s), so that $k_{2(\mathrm{diff})} = 8\times 10^9\ M^{-1}\ s^{-1}$. In a previous treatment [35] of the EC_{2i} case (which the behavior represented in Fig. 4 closely resembles, since eqn. (10) essentially remains at equilibrium) chemical irreversibility was observed, if the dimensionless parameter $k_2 c^\circ RT/Fv \geqslant 5$. For $v = 2000$ V s^{-1}, k_2 must be larger than $2\times 10^8\ M^{-1}\ s^{-1}$. Thus k_2 lies between 8×10^9 and 2×10^8 $M^{-1}\ s^{-1}$.

The reversible oxidation potential was estimated from the measured $E_{p/2}$ values and the above k_2-value range. If the heterogeneous electron-transfer kinetics are fast and k_2 is large relative to v (E_RC_{2i} case), the reversible oxidation potential can be obtained from eqn. (12) [35]:

$$E^{\circ\prime\prime} = E_{p/2} + (1.43 + \ln\ k_2 c^\circ RT/Fv)\,RT/3nF \tag{12}$$

At scan rates below 10 V s^{-1}, the shape of the oxidation wave matches that of the E_RC_{2i} case. For example, at 200 mV s^{-1}, $|E_{3/4} - E_{1/4}| = 32$ mV, compared to the expected value of 29 mV [29]. The range of possible values of k_2 derived earlier, (i.e., $2\times 10^6 \geqslant k_2 c^\circ RT/Fv \geqslant 5\times 10^4$ at 200 mV s^{-1}) and $E_{p/2} = +0.37$ V, gives a narrow range of possible values for $E^{\circ\prime\prime}$ ($E^{\circ\prime\prime} = E^{\circ\prime} + (RT/nF)\ln(K_1/(1+K_1))$) [29]: $+0.48 \leqslant E^{\circ\prime\prime} \leqslant +0.51$, on the assumption that the CE_RC_{2i} mechanism holds at 200 mV/s. The uncertainty in $E^{\circ\prime\prime}$ is thus reduced from previous work [11], which illustrates the utility of ultramicroelectrodes at fast sweep rates to obtain redox potentials for short lived species formed via heterogeneous electron transfer.

Studies in THF and HMPA

The electrochemistry of LiCp in THF and THF + HMPA mixtures has been studied previously [11]. Because HMPA solvates Li^+ effectively, ion pairs and clusters of the lithiated hydrocarbon are broken up. Electrochemical oxidations of carbanions in THF in the presence of HMPA show better reproducibility and less electrode fouling than in THF alone. Our studies involved mixtures of HMPA (at concentrations of ~ 20%) in THF. The CV oxidation wave gradually shifts towards more negative potentials with increasing HMPA concentrations (up to 20% HMPA), as reported previously [11].

A voltammogram of equimolar (10 mM) CpH + BuO^- at − 42 °C in THF + HMPA is shown in Fig. 7. A mechanism analogous to eqns. (6) and (7) with fast heterogeneous electron transfer can be assigned to this system (deprotonation of the CpH preceding the electrochemical oxidation, and followed by dimerization). The half peak potential shifts with v with a slope of 19.6 mV per scan rate decade (the anticipated slope at this temperature is 15.6 mV [29,35]). In contrast to previous reports [11] we found some electrode fouling to occur in this solvent during a bulk electrolysis experiment, and the electrode became passivated after a charge equivalent to an $n_{app} \approx 0.2$ electrons/molecule were passed. The color of the solution at this point closely resembled that of the red ammonia solution described earlier. However, deprotonation of the initial product of the oxidation (dihydrofulvalene) cannot have occurred in this solvent on the time scale of the cyclic voltammogram, since no waves other than Cp^- were seen on the second and subsequent scans.

Two methyl analogues of Cp^- (methylcyclopentadienide, $MeCp^-$, and 1,2,3,4,5-pentamethylcyclopentadienide, Me_5Cp^-) were examined to determine what effects steric hindrance might have on the electrode reaction mechanism. The CV oxidation of Li^+MeCp^- in THF + HMPA is shown in Fig. 8a. The oxidation wave shows many of the same characteristics as that of Cp^- oxidation (e.g., Fig. 2). The peak shows no reversal wave, because of the effects of the following reaction. The waveshape shows $E_p - E_{p/2} = 70$ mV, which implies a moderately fast heterogeneous electron transfer [36]. The half peak potential is at a more negative potential

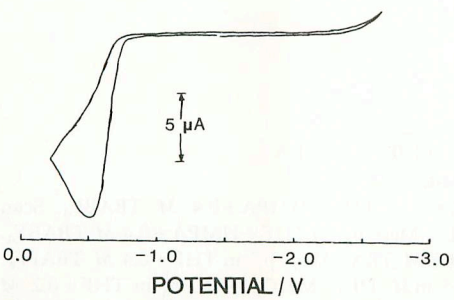

Fig. 7. Cyclic voltammogram of 10 mM CpH + K^+ t-BuO^- in THF + 20% HMPA at − 42 °C. Scan rate = 100 mV s^{-1}.

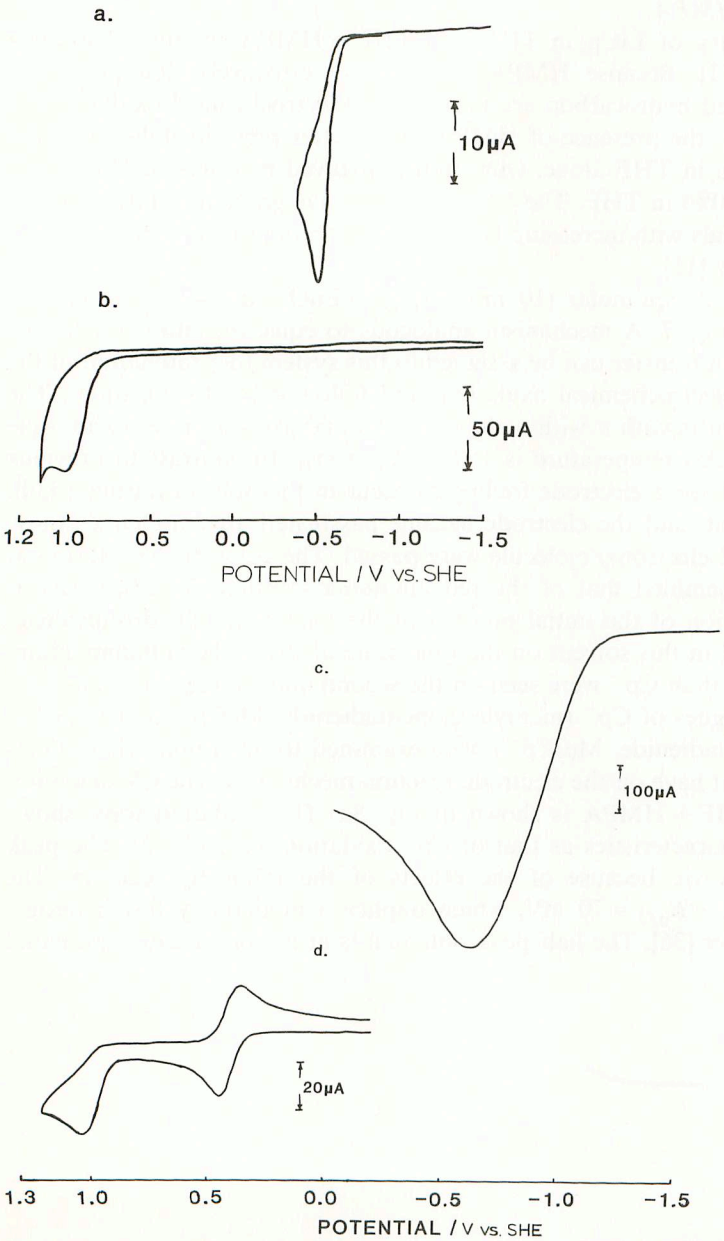

Fig. 8. (a) Cyclic voltammogram of 5 m*M* $Li^+ MeCp^-$ in THF + HMPA + 0.4 *M* $TBABF_4$. Scan rate = 100 mV s^{-1}. (b) Cyclic voltammogram of 5 m*M* $Li^+ Me_5Cp^-$ in THF + HMPA + 0.4 *M* $TBABF_4$. Scan rate = 100 mV s^{-1}. (c) Cyclic voltammogram of 90 m*M* $TBA^+ Me_5Cp^-$ in THF + 0.4 *M* $TBAPF_6$. Scan rate = 200 mV s^{-1}. (d) Cyclic voltammogram of 5 m*M* $TBA^+ Me_5Cp^- + KPF_6$ in THF + 0.2 *M* $TBAPF_6$. Scan rate = 200 mV s^{-1}. The reversible wave at + 0.40 V is due to 5 m*M* ferrocene, which was added as an internal reference.

(-0.58 V vs. SHE compared with -0.50 V for LiCp at $v = 200$ mV s^{-1}), perhaps because the electron donating effect of the methyl group shifts the $E°$ to less positive values. In contrast to this, the electrochemical oxidation of $Li^+Me_5Cp^-$ (Fig. 8b) in THF + HMPA occurs at a much more positive potential ($+1.00$ V vs. SHE). The oxidation wave of $Li^+Me_5Cp^-$ has the voltammetric characteristics of a totally irreversible charge transfer [37]: the half peak potential shifts 100 ± 10 mV per decade of scan rate, and $E_p - E_{p/2}$ is 160 ± 10 mV at 200 mV/s. This would correspond to an anodic transfer coefficient $(1-\alpha)n$ of 0.30 ± 0.03, for this oxidation reaction.

The extreme positive shift in the oxidation potential of $Li^+Me_5Cp^-$ compared to either Cp^- or $MeCp^-$ is surprising and somewhat puzzling. The peak potential for a totally irreversible charge transfer (at a given scan rate and temperature) depends primarily on the reversible potential $E°'$ and the heterogeneous electron-transfer rate constant $k°$, according to eqn. (13) [37]:

$$E_p = E°' - (RT/\alpha nF)\left[0.780 + \ln(D_0^{1/2}/k°) + \ln(\alpha nFv/RT)^{1/2}\right] \quad (13)$$

The observed waveform and scan rate behavior show that heterogeneous electron-transfer kinetics are at least partially responsible for the positive value of the peak potential. The most reasonable explanation for the effect is a combination of sluggishness in the heterogeneous electron transfer kinetics, and a positive shift in the standard oxidation potential. An explanation based purely on sluggishness in the heterogeneous electron-transfer rate is improbable, since from eqn. (13) an unreasonably small value of $k°$ ($\sim 10^{-10}$ cm^2 s^{-1}) would be required. On the other hand, chemical effects, such as ion pairing and clustering of the lithiated hydrocarbon, can be invoked to explain a positive shift in the standard oxidation potential.

It has been noted that lithiated hydrocarbons are more likely to aggregate than their sodium and potassium analogues, and that the reactivity of these species varies accordingly [2]. In a series of carbanions, aggregation would be least likely for the quaternary ammonium salt, and thus the electrochemical behavior would be attributable to a monomeric carbanion. The electrochemistry of tetra-n-butylammonium Me_5Cp^- ($TBA^+Me_5Cp^-$) was examined and compared to the other compounds.

The synthesis of a tetraalkylammonium salt of a cyclopentadienide has not been reported previously. $TBA^+Me_5Cp^-$ was synthesized in high yield from KMe_5Cp in THF according to eqn. (14) (see Experimental):

$$KMe_5Cp^- + TBAPF_6 \xrightarrow{THF} TBA^+Me_5Cp^- + KPF_6 \quad (14)$$

The electrochemical oxidation of $TBA^+Me_5Cp^-$ is shown in Fig. 8c. The broadness in the wave ($E_p - E_{p/2} = 250$ mV) implies a totally irreversible electron transfer, with $(1-\alpha)n = 0.2$. The half-peak potential (-0.90 V vs. SHE) is more negative than either Cp^- or $MeCp^-$, as expected from the inductive effects of the methyl groups on the standard oxidation potential.

As further evidence of the effect of the counterion on the oxidation potential of Me_5Cp^-, the voltammetry of 5 m*M* $TBA^+Me_5Cp^-$ in THF + 0.2 *M* $TBAPF_6$ in the presence of equimolar KPF_6 is shown in Fig. 8d. The oxidative half-peak potential is virtually identical to that of $LiMe_5Cp$, as seen in Fig. 8b. Thus, the lithium and potassium salts of Me_5Cp^- exhibit significantly different electrochemistry from $TBA^+Me_5Cp^-$, which may be ascribed to clustering or ion pairing of these species in solution.

The electrochemical results outlined above lead to two conclusions concerning the oxidation behavior of cyclopentadienides in THF + HMPA mixtures: (1) Substitution of the protons on the ring with methyl groups may increase the electron density in the π system, which decreases the oxidation potential for methylated cyclopentadienides. (2) Oligomers of the alkali metal salts of cyclopentadienides may exist in solution, and these oligomers are more difficult to oxidize. The oligomers may be solvated and broken up by the addition of HMPA, but in the case of Li and KMe_5Cp, the electrochemistry suggests clustering even in a 20% HMPA + THF solution.

The stabilization of Li and KMe_5Cp by the aggregation must be considerable, since the observed oxidation potential is nearly 2 V positive of an ionic Me_5Cp^-. Thus, the inability of HMPA to solvate the cluster may be explained in terms of the high stability of the aggregate. A more detailed study into the solution structures of $LiMe_5Cp$ should be carried out, especially since our results conflict with the expectation that the increased steric hindrance in this molecule should restrict any clustering.

CONCLUSIONS

The studies suggest that the electrochemical reduction of CpH in ammonia is preceded by a strong interaction with the solvent. An analogous mechanism is not available in non-basic media, and no reduction process is observed.

The oxidation of these molecules occurs via CE_qC_{2i} kinetics for CpH derivatives in ammonia, and E_qC_{2i} kinetics for all Cp^- derivatives generally. A second-order following reaction was observed for the Cp^- derivatives, despite the expectation [38] that the cyclopentadienyl radical undergoes a Jahn–Teller distortion (a first-order process). However, calculations have shown [39] that interconversion between all C_{2v} isomers is very rapid at ambient temperature, thus the rate limiting step following electrooxidation is second-order.

The methylation of the C_5-ring decreases the oxidation potential of the cyclopentadienide, possibly due to increased electron density in the π system caused by the inductive effects of the methyl groups. We also find that despite the steric hindrance in the permethylated compound, Li and KMe_5Cp form a very stable cluster which is hard to oxidize electrochemically, or to solvate.

The synthesis and electrochemistry of a quaternary ammonium salt of a cyclopentadienide was examined. The oxidation potential of $TBA^+Me_5Cp^-$ suggests the molecule is monomeric in solution, analogous to HMPA-solvated LiCp compounds.

The reactivity of this compound may be of interest in the synthesis of new organometallic complexes. For example, in previously reported syntheses of lanthanide metal metallocenes using alkali metal cyclopentadienides, the counterion of the Cp^- reagent is always incorporated into the final product [21]. In contrast, a quaternary ammonium salt would not be expected to react in this fashion. Furthermore, we have found that the $TBA^+Me_5Cp^-$ is far more soluble than KMe_5Cp (up to 1 *M*) in THF. Thus, this salt may be a convenient and useful reagent in organometallic synthesis.

Electrode fouling on the bulk electrolysis time scale limits the utility of electrooxidation of cyclopentadienides for generating macroquantities of pentafulvalenes. Dilute solutions of neutral fulvalene and dihydrofulvalene are available by the oxidation of Cp^- in ammoniacal and THF solution, respectively. This may be of use for in situ generation of these molecules.

Finally, the use of ultramicroelectrodes to explore fast second-order reaction pathways was successful even though chemical reversibility was not observed at the fastest scan rates. The range of possible values for $E^{\circ\prime}$ for the $Cp^{-/0}$ couple was reduced considerably compared to the previous estimates.

ACKNOWLEDGEMENTS

This work was carried out under a National Science Foundation grant (CHE 8402135). We would also like to thank Dr. Stephen Feldberg for his helpful comments concerning this manuscript.

REFERENCES

1 M. Herlem, F. Bobilliant and A. Thiebault in A.J. Bard and H. Lund (Eds.), Encyclopedia of Electrochemistry of the Elements, Vol. 11, Marcel Dekker, New York, 1978, p. 1.
2 F.A. Cotton and G. Wilkinson, Advanced Inorganic Chemistry, A Comprehensive Text, Wiley, New York, 1980, p. 269.
3 W. Hückel and R. Schwen, Chem. Ber., 89 (1956) 150.
4 K. Ziegler, H. Froitzheim-Kühlhorn and K. Hafner, Chem. Ber., 89 (1956) 434.
5 J. Thiele, Ber. Dtsch. Chem. Ges., 33 (1900) 666; 34 (1901) 68.
6 M.D. Hawley in P.T. Kissinger and W.R. Heineman (Eds.), Laboratory Technique in Electroanalytical Chemistry, Marcel Dekker, New York, 1984, p. 463.
7 J.R. Jezorek, A. Lagu, T.M. Seigel and H.B. Mark, J. Org. Chem., 38 (1973) 788.
8 A.G. Davies and J. Lusztyk, J. Chem. Soc., Chem. Commun., (1980) 554 and references therein.
9 J.O. Howell and R.M. Wightman, Anal. Chem., 56 (1984) 524.
10 R. Breslow and S. Mazur, J. Am. Chem. Soc., 95 (1973) 584.
11 B. Jaun, J. Schwarz and R. Breslow, J. Am. Chem. Soc., 102 (1980) 5741.
12 R.D. Moulton and A.J. Bard, Organometallics, 7 (1988) 351.
13 W. von E. Doering, Theoretical Organic Chemistry. The Kekulé Symposium, Butterworths, London, 1959.
14 W. Rutsch, A. Escher and M. Neuenschwander, Chimia, 37 (1983) 160.
15 A. Escher and M. Neuenschwander, Angew. Chem., Int. Ed. Engl., 23 (1984) 973.
16 A.G. Davies, J.R.M. Giles and J. Lusztyk, J. Chem. Soc. Perkin Trans., 2, 3 (1981) 747.
17 R. Brand, H.-P. Krimmer, H.J. Lindner, V. Sturm and K. Hafner, Tetrahedron Lett., 23 (1982) 5131.

18 K.P.C. Vollhardt and T.W. Weidman, Organometallics, 3 (1984) 82 and references therein.
19 R.M. Crooks and A.J. Bard, J. Phys. Chem., 91 (1987) 1274.
20 J.C. Smart and C. Curtis, Inorg. Chem., 16 (1977) 1788.
21 H. Schumann, I. Albrecht, J. Loebel, E. Hahn, M.B. Hossain and D. van der Helm, Organometallics, 5 (1986) 1296.
22 R.D. Moulton, T.W. Weidman, K.P.C. Vollhardt and A.J. Bard, Inorg. Chem., 25 (1986) 1846.
23 E. Garcia, J. Kwak and A.J. Bard, Inorg. Chem., in press.
24 W.M. Koepp, H. Wendt and H. Strehlow, Z. Electrochem., 64 (1960) 483.
25 A.M. Bond, E.A. McLennan, R.S. Stojanovic and F.G. Thomas, Anal. Chem., 59 (1987) 2853.
26 A. Streitwieser and L.L. Nebenzahl, J. Am. Chem. Soc., 98 (1976) 2188.
27 D.T. Sawyer and J.L. Roberts, Experimental Electrochemistry for Chemists, Wiley, New York, 1974, p. 61.
28 J. Badoz-Lambling and M. Herlem, Bull. Soc. Chim. Fr., 31 (1964) 90.
29 R.D. Moulton, A.J. Bard and S.W. Feldberg, J. Electroanal. Chem., 256 (1988) 291.
30 M.A. Cooper, D.D. Elleman, C.D. Pearce and S.L. Manatt, J. Chem. Phys., 53 (1970) 2343.
31 T. Birchall and W.L. Jolly, J. Am. Chem. Soc., 87 (1965) 3007.
32 C.L. Perrin, J. Am. Chem. Soc., 108 (1986) 6807 and references therein.
33 K.V. Ingold in J.K. Kochi (Ed.), Free Radicals, Vol. 1, Wiley, New York, 1973, p. 39.
34 R.B. Bird, W.E. Stewart and E.N. Lightfoot, Transport Phenomena, Wiley, New York, 1960, p. 29.
35 M.L. Olmstead, R.G. Hamilton and R.S. Nicholson, Anal. Chem., 41 (1969) 260.
36 D.H. Evans, J. Phys. Chem., 76 (1972) 1160.
37 R.S. Nicholson and I. Shain, Anal. Chem., 36 (1964) 706.
38 P.J. Barker, A.G. Davies and M.-W. Tse, J. Chem. Soc., Perkin Trans. 2, (1980) 941.
39 See, for example, L.C. Snyder, J. Chem. Phys., 33 (1960) 619.